Investigation of Ideal-MHD Stable Scenario for Plasma Current Ramp-Up with No Magnetic Flux Consumption in JT-60SA*)

Takuma WAKATSUKI, Takahiro SUZUKI, Nobuhiko HAYASHI,
Junya SHIRAISHI, Shunsuke IDE, Hirotaka KUBO and Yuichi TAKASE[1)]

Japan Atomic Energy Agency, Naka 311-0193, Japan
[1)] *University of Tokyo, Kashiwa 277-8561, Japan*

(Received 27 November 2015 / Accepted 18 March 2016)

Feasibility of plasma current ramp-up in JT-60SA with no additional central solenoid (CS) flux consumption after the initial plasma formation has been investigated using an integrated modeling code suite (TOPICS). In our previous study, we developed a scenario in which the plasma current is ramped-up from 0.6 MA to 2.1 MA with no additional CS flux consumption by overdriving the plasma current using neutral beams (NB) and electron cyclotron (EC) waves. While the density profiles were prescribed in the previous study, in this study, we introduce a particle transport model according to the experimental results of JT-60U. It is shown that an internal transport barrier (ITB) can be obtained and the plasma current can be overdriven even if the particle transport is solved. The plasma current is ramped up in 330 s without CS flux consumption using 17 MW of NB and 3 MW of EC when the electron density is approximately 70% of the Greenwald limit. Although low-n ideal MHD modes are stable, an infinite-n ballooning mode is unstable in this scenario. The latter mode is presumably harmless, but to ensure the stability we investigate the pressure and the current profile controllability when the plasma current is overdriven. As a result, the infinite-n ballooning mode is shown to be stable when a broad pressure profile and a locally optimized magnetic shear are obtained using 2 MW of on-axis N-NB, 2 MW of off-axis N-NB, 4 MW of co-tangential P-NB and 7MW of EC with the electron density 30% of the Greenwald limit.

Keywords: plasma current overdrive, non-inductive, MHD stability, TOPICS, MARG2D, JT-60SA, simulation

DOI: 10.1585/pfr.11.2403068

1. Introduction

If the amount of magnetic flux swing capability of central solenoid (CS) required for plasma current ramp-up is reduced, a strong constraint on the tokamak reactor designs is relaxed. Current start-up and/or ramp-up operations without CS flux consumption were demonstrated in many tokamaks, e.g. JT-60U [1], PLT [2], DIII-D [3]. Nonetheless, the experimental data on large tokamaks which can confine reactor relevant high pressure plasmas are not sufficient to ensure the extrapolability to the reactor plasma.

We have investigated reduction of the CS flux required in the current ramp-up phase in JT-60SA using an integrated modeling code, TOPICS suite [4]. In the previous study on current ramp-up with reduced CS flux consumption in JT-60SA, we developed a scenario in which the plasma current is ramped-up from 0.6 MA to 2.1 MA in 150 s without additional CS flux consumption by overdriving the plasma current using neutral beams (NB) and electron cyclotron (EC) waves [5]. Here, the plasma current overdrive means that the non-inductive current, which is a sum of a bootstrap current, NB driven current and EC driven current, exceeds the plasma current. The prescribed density profiles which had strong internal transport barrier (ITB) and H-mode pedestal were used in previous study, however, the pressure profiles were strongly dependent on these prescribed density profiles. If the particle transport is solved, the width and the location of the density ITB might be different from the prescribed density profiles. Therefore, in this study we investigate the possibility of modification of the pressure profiles using the heating and current drive (H & CD) actuators in JT-60SA by solving both the particle transport and the thermal transport. In particular, if local pressure gradient becomes too steep, a localized mode such as an infinite-n ballooning mode might be unstable. In fact, the infinite-n ballooning mode is unstable in the previous study. Therefore, we investigate pressure profile controllability in order to avoid infinite-n ballooning mode stability limit in addition to low-n mode stability which can be studied by an ideal MHD stability code MARG2D.

This article is organized as follows. In section 2, characteristics of the modeling tools and the heating current drive configurations of JT-60SA are described. An introduced particle transport model is also described in this section. The example of the current ramp-up scenario with no

author's e-mail: wakatsuki.takuma@qst.go.jp
*) This article is based on the presentation at the 25th International Toki Conference (ITC25).

CS flux consumption which is calculated according to the particle and heating transport model is described in section 3. Controllability of pressure profile under the condition that the plasma current is overdriven is shown in section 4, and conclusions are given in section 5.

2. Modeling Tools and Assumed Experimental Conditions

TOPICS is an integrated modeling code suite and its main part solves the 1-D transport equations [6] in accordance with the 2-D free boundary equilibrium. Several turbulent models can be used for the integration of the anomalous heat transport in TOPICS. Among them, we use CDBM model which demonstrated its ability to reproduce plasma profiles with ITB in JT-60U [7, 8]. As for the particle transport calculation, we assume that the anomalous particle diffusivity is proportional to the thermal diffusivity according to experimental results of JT-60U. In the reversed shear plasmas on JT-60U, the effective particle diffusivity in the ITB region was estimated to be 0.04-0.2 times the ion thermal diffusivity when only the diffusion term was considered [9]. Thus, we assume an effective anomalous particle diffusivity $D_{\mathrm{ano}} = 0.2 \times \chi_{\mathrm{CDBM,i}}$ and calculate the particle transport assuming that the particle diffusivity is a sum of neoclassical and anomalous diffusivities with zero anomalous particle pinch velocity. The neoclassical diffusivity is needed for including a strong neoclassical diffusion inside the reversed shear region. Particle sources are NBI and the edge gas puff. The volume averaged density is feedback controlled by the edge gas puff.

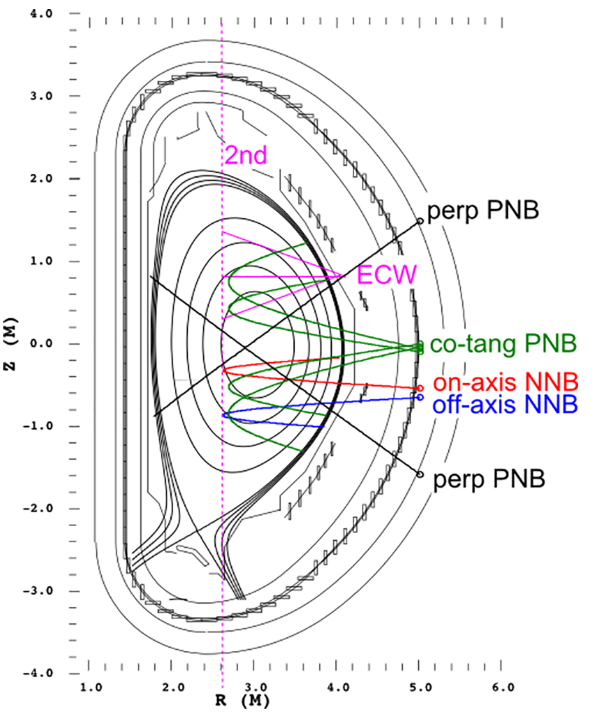

Fig. 1 NB trajectories and EC ray trajectories with a plasma equilibrium. The NB trajectories of on-axis N-NB, off-axis N-NB, co-tangential P-NB and perpendicular P-NB are shown. The locations of the stabilizing plate, the vacuum vessel, the TF coil are also shown. EC ray trajectories with poloidal angles −20°, 0° and +20° are shown.

JT-60SA will be equipped with two tangential negative ion based neutral beams (N-NB), 24 positive ion based neutral beams (P-NB) and a steerable EC wave launcher as shown in Fig. 1. The beam energy of the N-NB will be 500 keV while that of the P-NB will be 85 keV. One of the N-NB will be injected on-axis and the other will be off-axis to the plasma magnetic axis, which can be used to modify the current profile, and each beam power will be 5 MW. There will be three groups in the P-NB, which will be co-tangential beams, counter-tangential beams and perpendicular beams to the plasma current. Co- and counter-tangential beams consist of four beams with 1 MW power each, respectively, and perpendicular beams consist 16 beams with 1 MW power each. The maximum power of the EC wave will be 7 MW.

3. Plasma Current Overdrive

Figure 2 is one of the results of the ramp-up scenario simulation. It is shown that the plasma current can be overdriven using the H & CD system of JT-60SA during the plasma current ramp-up even in the simulation in which particle transport is solved. The plasma current is ramped up from 0.6 MA to 2.1 MA without a flux consumption of CS and equilibrium field (EF) coils. It takes 330 s (from 5 s to 335 s) for the current ramp-up in this scenario. This duration is longer than the discharge duration of JT-60SA (100 s) and the duration in the previous study (150 s) [5], however, if more NB power is injected to shorten the ramp-up duration, the location of ITB moves outwards in minor radius and the confinement quality becomes too good. Then, plasma beta becomes too high and the plasma becomes unstable.

At the low current (0.6 MA) phase, only co-tangential P-NB and EC can be used because shine through losses of on- and off-axis N-NBs and perpendicular P-NB are large. Therefore, the plasma current is overdriven using co-tangential P-NB and EC from 5 s. The toroidal injection angle of EC wave is 10 degrees in the co-direction and EC is locally absorbed around $\rho = 0.45$. On the other hand, once the plasma current exceeds 1 MA and the electron density becomes higher than $1 \times 10^{19}\ \mathrm{m}^{-3}$, shine through losses of on- and off-axis N-NBs and perpendicular P-NB become less than 10%. In this scenario, we try not to use EC in the high current phase because a localized EC current drive might be required for other purpose such as a stabilization of neoclassical tearing modes.

Time evolution of the density profile, the temperature profile and the safety factor profile are shown in Fig. 3. The density and the temperature profiles at the edge region ($\rho \geq 0.85$) is prescribed in order to assume appropri-

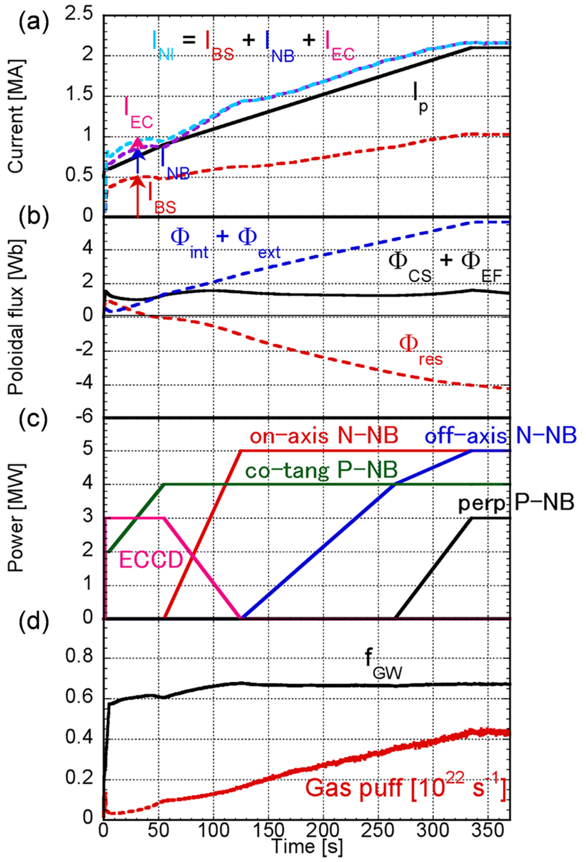

Fig. 2 TOPICS simulation of a current ramp-up scenario from 0.6 MA to 2.1 MA without CS flux consumption. Time evolution of (a) the plasma current (I_p), non-inductive current (I_{NI}) and its three components, (b) CS and EF flux consumption and its inductive and resistive component, (c) input powers used for the auxiliary heating and current drive, (d) the fraction of the electron density to the Greenwald density limit (f_{GW}) and the gas puff rate.

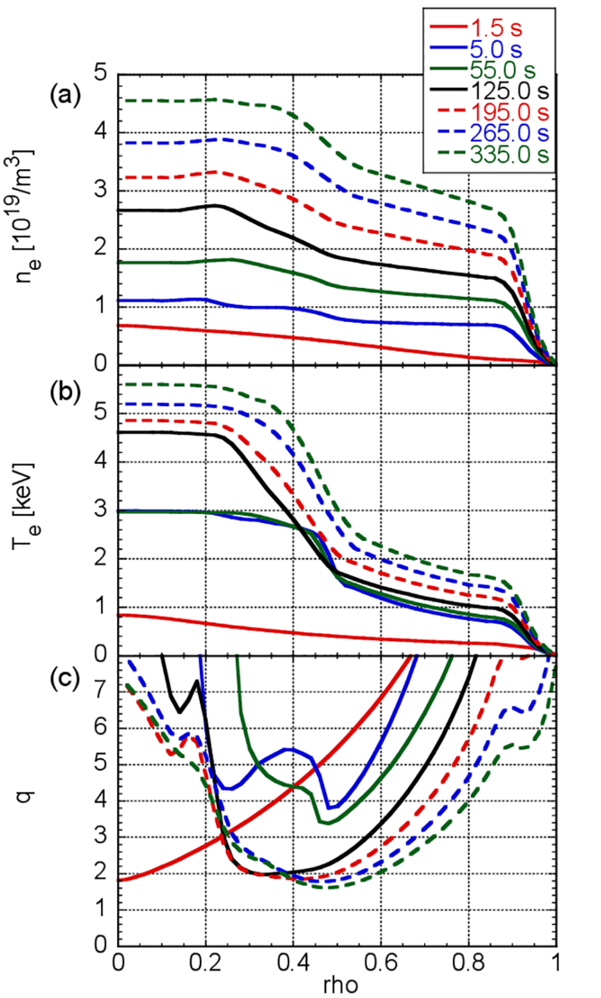

Fig. 3 Time evolutions of (a) the density profile, (b) the electron temperature profile and (c) the safety factor q in the scenario shown in Fig. 2.

ate pedestal pressure height and width in accordance with the scaling law by Cordey et al [10] and EPED-width scaling [11], respectively. We assume that the L-H transition takes place around 5 s because the threshold power is 1.6 MW. The current driven by NB and EC and the bootstrap current consists a large off-axis current. Then, the reversed shear configuration which has the minimum value of a safety factor (q) at an off-axis location is formed as shown in Fig. 3 (c). As a result, the ITBs in the density and the temperature are formed as shown in Fig. 3 (a,b) because the anomalous transport is reduced at the region of the weak or negative magnetic shear in CDBM model.

Nonetheless, the strength of ITB in the density is weaker than the prescribed profiles used previously as shown in Fig. 4 (a). This is because the particle source by NB which can provide ions in the plasma core region is small as shown in Fig. 4 (b). As a result, the bootstrap current decreases compared with the previous case. Then, the electron density is kept lower in this scenario because it was shown that the non-inductive current increases as the electron density decreases. The fraction of the electron density to the Greenwald density limit (f_{GW}) is kept approximately 0.6 - 0.7 throughout the current ramp-up. If we consider a pellet injection, stronger density ITB might be attained, however, ideal MHD modes are thought to be unstable when ITB becomes stronger as shown later. Therefore we don't consider a pellet injection in this study.

The stabilities of low-n (n = 1 - 3) ideal MHD modes are investigated using a linear ideal MHD stability code MARG2D [12]. These modes are stable if we assume a perfectly conducting wall is placed at the location of a vacuum vessel and a stabilizing plate of JT-60SA. On the other hand, a normalized pressure gradient $\alpha = -(2\mu_0 R q^2/B^2)\,\mathrm{d}p/\mathrm{d}r$ is larger than the stability limit of an infinite-n ballooning mode α_{crit} which can be calculated from the ballooning equation [13] at 335 s as shown in Fig. 5. A localized infinite-n ballooning mode might not cause a plasma disruption, however, can lead to a degradation of ITB. In addition, a localized mode near ITB which causes a minor collapse might be excited when the local

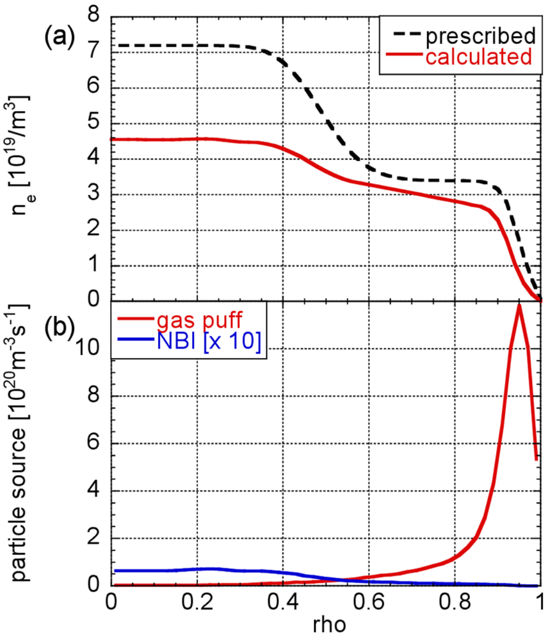

Fig. 4 (a) Comparison of the calculated density profile and the prescribed density profile used in previous study [5] at the current flat top. (b) Profiles of ion sources by the gas puff and NBI. Note that NBI particle source shown here is magnified by 10 times.

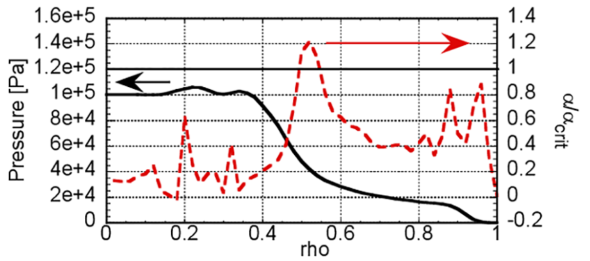

Fig. 5 Profiles of the total plasma pressure (black, solid) and $\alpha/\alpha_{\mathrm{crit}}$ (red, broken) at 335 s in the scenario shown in Fig. 2.

pressure gradient is near the stability limit of infinite-n ballooning mode [14]. Therefore, we try to modify the pressure profile in order to avoid the infinite-n ballooning instability.

4. Pressure Profile Control

In order to investigate the pressure profile controllability under the condition that the plasma current should be overdriven, we calculate many plasma current ramp-up scenarios with different H & CD inputs and electron densities. In these cases, durations of the plasma current ramp-up is reduced to 25 s in order to reduce computational cost. Although the CS flux is consumed in this faster ramp-up case, if the plasma current is shown to be overdriven in this calculation, CS-less current ramp-up becomes possible at sufficiently slow ramp-up rate using the same H & CD input. As for the representative time step, pressure profiles at the beginning (5 s) and the end (30 s) of the plasma current ramp-up is mainly investigated.

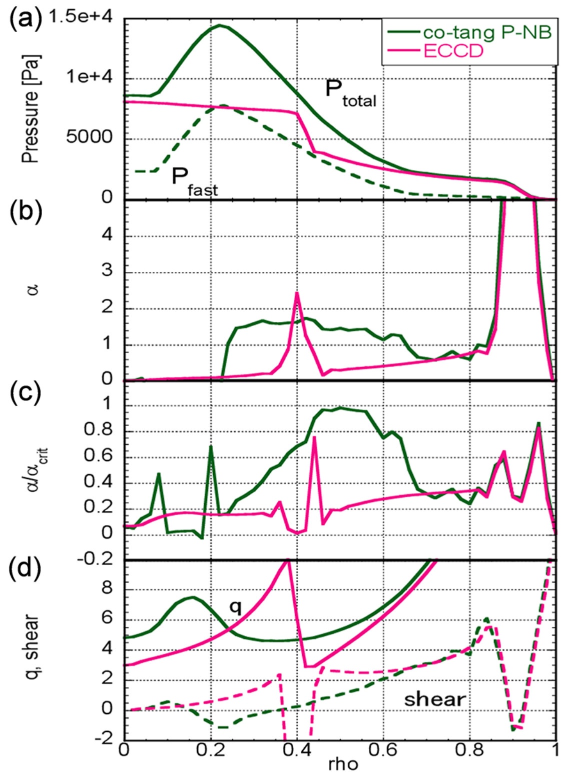

Fig. 6 Profiles of (a) the total plasma pressure (solid) and the fast ion pressure (broken), (b) the normalized pressure gradient α, (c) the ratio of α over α_{crit} and (d) the safety factor q (solid) and the magnetic shear (broken) at 5 s and $I_{\mathrm{p}} = 0.6$ MA. Pink and Green lines represent the cases 3.02 MW of co-tangential P-NB and 7.00 MW of EC are injected, respectively.

As is mentioned in the previous section, only tangential P-NB and EC can be used at the low current (0.6 MA) phase before the plasma current ramp-up. Figure 6 shows differences in the profile of pressure, α, $\alpha/\alpha_{\mathrm{crit}}$, q and a magnetic shear ($s = (\rho/q)\mathrm{d}q/\mathrm{d}\rho$) when 3.02 MW of co-tangential P-NB or 7.00 MW of EC are injected to the plasma with the electron density which is approximately 60% of the Greenwald limit. While the P-NB input power (3.02 MW) was lower than a half of the EC input power (7.00 MW), the non-inductive current driven by P-NB (0.64 MA) was almost the same as that by EC (0.67 MA) because co-tangential P-NB has higher current drive efficiencies than EC. When 3.02 MW of co-tangential P-NB is applied, even though the pressure becomes higher and α becomes larger in a wide region due to a large fast ion pressure, $\alpha/\alpha_{\mathrm{crit}}$ is less than unity all over the plasma. However, if 4 MW of co-tangential P-NB is injected, the ballooning stability criterion is violated. Therefore, co-tangential P-NB can overdrive the plasma current more efficiently than EC, but the input power should be kept sufficiently low in order to prevent the infinite-n ballooning mode from being unstable.

On the other hand, α becomes large at a localized region when 7 MW of EC is applied. Although α of the EC case is larger than that of the P-NB case at this narrow region, α/α_{crit} is smaller. This is because the magnetic shear becomes negative at this region due to the localized current drive by EC. An infinite-n ballooning mode is stabilized when shear becomes small or negative, therefore, α_{crit} becomes large. As a result, the plasma current is overdriven without violating the ballooning stability criterion using 7 MW of EC. However, 7 MW is the upper limit of available EC power of JT-60SA. Therefore, if plasma density is increased to 100% of the Greenwald limit, the current drive efficiency decreases and plasma current cannot be overdriven by EC.

At the high current (2.1 MA at 30 s) phase, on- and off-axis N-NBs can be used for the current drive in addition to co-tangential P-NB. In Fig. 7 (a), the non-inductive currents driven by co-tangential P-NB, on-axis N-NB or off-axis N-NB are compared with two densities which are the same volume averaged density as the cases in Sec. 3 ($f_{GW} \sim 0.6$) and half density of it ($f_{GW} \sim 0.3$). In general, more non-inductive currents can be driven at low densities and on- and off-axis N-NBs can drive the non-inductive current more efficiently than co-tangential P-NB as already discussed in the previous paper. Figure 7 (b) shows the dependence of $\max(\alpha/\alpha_{crit})$ on the non-inductive current. In general, $\max(\alpha/\alpha_{crit})$ increases as the density decreases with the same input power because the slowing down time of fast ions becomes longer and the fast ion pressure increases as shown in Fig. 7 (c).

However $\max(\alpha/\alpha_{crit})$ is not much depend on the density if we compare $\max(\alpha/\alpha_{crit})$ in cases that the almost same non-inductive current is driven by a specific H & CD source as shown in Fig. 7 (b). This is because almost the same fast ion populations are needed to obtain the same non-inductive currents. On the other hand, $\max(\alpha/\alpha_{crit})$ can be decreased by using co-tangential P-NB rather than N-NBs. Therefore, it is better to use co-tangential P-NB preferentially. However, an available power of co-tangential P-NB is limited to 4 MW. Lower density operations are preferable because a larger non-inductive current can be driven by 4 MW of co-tangential P-NB and required additional powers of N-NBs for the plasma current overdrive can be reduced.

In Fig. 8, the pressure profiles are compared when the plasma current is slightly overdriven by 6.42 MW of on-axis N-NB, 7.11 MW of off-axis N-NB or 11.04 MW of co-tangential P-NB with the volume averaged density half of the case in Sec. 3. In all the cases, the non-inductive current is kept almost same (the difference is less than 5%). Infinite-n ballooning modes become unstable at the tail of fast ion profiles in on- and off-axis N-NB cases. On the other hand, pressure gradient becomes less steep with co-tangential P-NB and α/α_{crit} becomes less than unity.

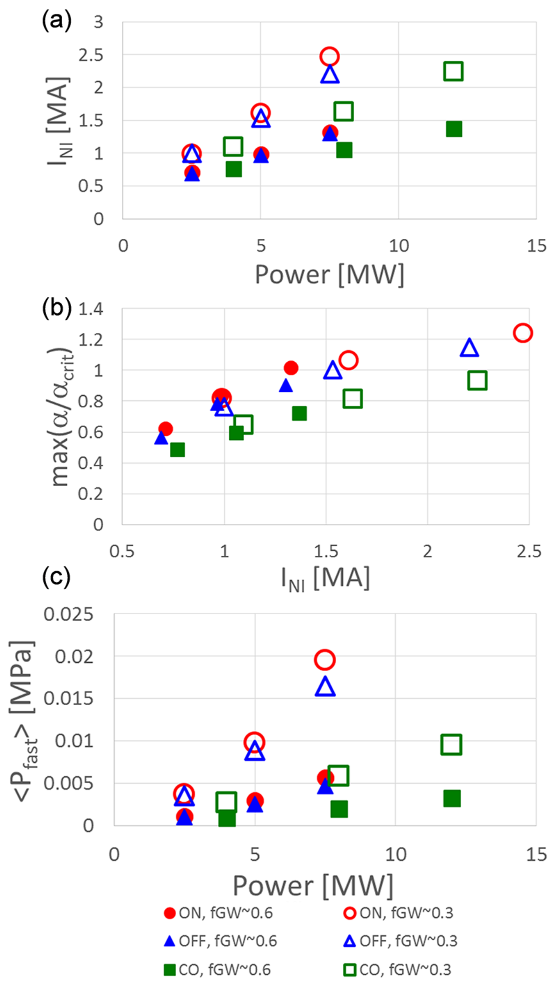

Fig. 7 Dependences of (a) the non-inductive driven current on input powers, (b) $\max(\alpha/\alpha_{crit})$ on the non-inductive driven current and (c) volume averaged pressure on input powers. Closed and open symbols stand for cases with the densities which are the same volume averaged density as the cases in Sec. 3 ($f_{GW} \sim 0.6$) and the half density of it ($f_{GW} \sim 0.3$), respectively. Circles, triangles and squares represent the cases on-axis N-NB and off-axis N-NB and co-tangential P-NB are used, respectively.

Therefore, the plasma current can be overdriven without violating the ballooning stability criterion if 11.04 MW of co-tangential P-NB is available at JT-60SA. However, only 4 MW of co-tangential P-NB is available, therefore, on- and/or off-axis N-NBs should be additionally used in order to overdrive the plasma current.

If on- and off-axis N-NBs are injected simultaneously with a same total input power, the pressure gradient can be reduced while almost the same non-inductive current is driven. Therefore, it is better to use 4 MW of co-tangential P-NB with two N-NBs with a necessary power for overdrive in order to avoid steep pressure gradient. However, even if 4 MW of co-tangential P-NB, 2 MW of on-axis N-NB and 2 MW of off-axis N-NB are used, α/α_{crit} exceeds unity at the tail of the fast ion profile. Then, a localized EC

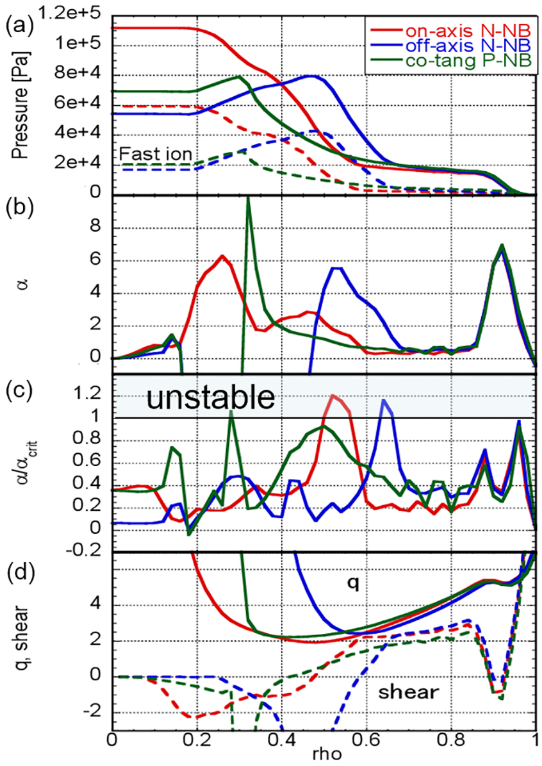

Fig. 8 Profiles of (a) the total plasma pressure (solid) and the fast ion pressure (broken), (b) the normalized pressure gradient α, (c) the ratio of α over α_{crit} and (d) q (solid) and the magnetic shear (broken) at 30 s and I_p = 2.1 MA. Red, blue and Green lines represent the cases 6.42 MW of on-axis N-NB, 7.11 MW of off-axis N-NB and 11.04 MW of co-tangential P-NB are injected, respectively.

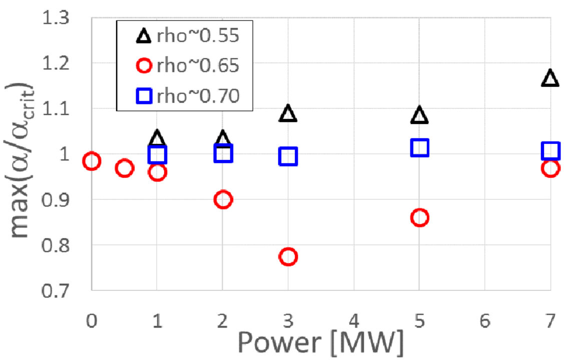

Fig. 9 Dependences of max(α/α_{crit}) on the input EC power on 3 different absorption positions (black triangle: $\rho \approx 0.55$, red circle: $\rho \approx 0.65$, blue square: $\rho \approx 0.70$).

current drive is used in order to stabilize the infinite-n ballooning mode because α_{crit} becomes large if the magnetic shear is reduced. As shown in Fig. 9, if an appropriate EC power is applied to drive a current at just outside of the tail of the fast ion profile, α/α_{crit} becomes below unity. As a result, the plasma current overdrive becomes possible under the condition that the infinite-n ballooning mode is stable as shown in Fig. 10.

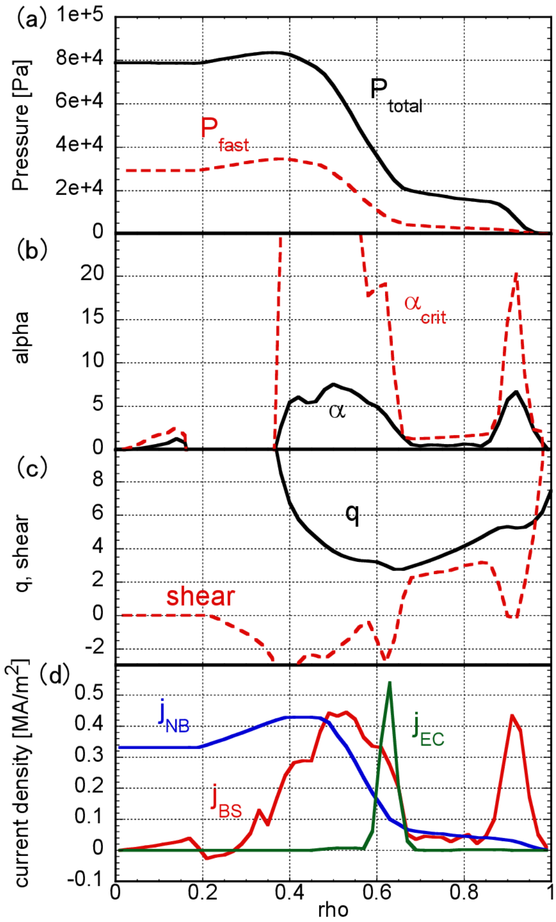

Fig. 10 Profiles of (a) the total plasma pressure (black, solid) and the fast ion pressure (red, broken), (b) α (black, solid) and α_{crit} (red, broken), (c) q (black, solid) and the magnetic shear (red, broken) , and (d) the bootstrap current density (red), the NB driven current density (blue) and the EC driven current density (green) at 30 s and I_p = 2.1 MA when 2 MW of on-axis N-NB, 2 MW of off-axis N-NB, 4 MW of co-tangential P-NB and 7 MW of EC are injected simultaneously.

5. Conclusions

We have shown that the plasma current can be ramped-up from 0.6 MA to 2.1 MA without additional CS flux consumption using TOPICS simulation in which particle and heat transport is solved according to empirical models based on the experimental results of JT-60U. Even though, ITB in the density is weaker than the previous simulation using prescribed density profiles and the bootstrap current decreases, the plasma current can be overdriven within H & CD capability of JT-60SA (17 MW of NB and 3 MW of EC) if the density is decreased to $f_{GW} \sim 0.7$. The current ramp-up rate should be very slow and it takes 330 s for the current ramp-up from 0.6 MA to 2.1 MA. This duration is longer than discharge duration of JT-60SA, however, even lower power and slower rate current ramp-up might be required because the infinite-n ballooning mode is unstable in this scenario.

In order to stabilize the infinite-n ballooning mode, the pressure profile control to obtain less steep pressure gradient is investigated under the condition that the plasma current is overdriven. At the low current (0.6 MA) phase, the plasma current can be overdriven without violating the ballooning stability criterion using either 3 MW of co-tangential P-NB or 7 MW of EC with the electron density which is approximately 60% of the Greenwald limit. Even though co-tangential P-NB can overdrive 0.6 MA with a smaller input power than EC, the pressure gradient becomes steep in wider region and the ballooning mode becomes unstable if a too much power is injected. At the high current (2.1 MA) phase, a less steeper pressure profile can be obtained when 2 MW of on-axis N-NB, 2 MW of off-axis N-NB and 4 MW of co-tangential P-NB is used simultaneously and the electron density is reduced to $f_{\mathrm{GW}} \sim 0.3$. However, the infinite-n ballooning mode is still unstable at the tail of the fast ion profile. Then a localized EC current drive is applied at just outside of the tail of the fast ion profile in order to stabilize the ballooning mode by reducing the magnetic shear. As a result, it is shown that the plasma current can be overdriven under the condition that the infinite-n ballooning mode is stable in addition to low-n ideal MHD modes if the pressure and the current profiles are properly controlled. The required duration for CS-less current ramp-up is estimated to be longer than 500 s if the optimized H & CD input as shown in Fig. 10 is used.

Aknowledgement

The authors wish to thank Dr. Y. Kamada for fruitful discussion and advice on the basis of experimental knowledge in JT-60U. This work is supported by JSPS Grant-in-Aid for Research Activity Start-up 26889069 and carried out under the National Centralized Tokamak Collaborative Research Program between the University of Tokyo and JAEA. This work was carried out using the HELIOS supercomputer system at International Fusion Energy Research Centre, Aomori, Japan, under the Broader Approach collaboration between Euratom and Japan, implemented by Fusion for Energy and JAEA.

[1] S. Shiraiwa *et al.*, Phys. Rev. Lett. **92**, 035001 (2004).
[2] F. Jobes *et al.*, Phys. Rev. Lett. **52**, 1005 (1984).
[3] J.A. Leuer *et al.*, Nucl. Fusion **51**, 063038 (2011).
[4] N. Hayashi *et al.*, Phys. Plasmas **17**, 056112 (2010).
[5] T. Wakatsuki *et al.*, Plasma Phys. Control. Fusion **57**, 065005 (2015).
[6] M. Kikuchi and M. Azumi, Plasma Phys. Control. Fusion **37**, 1215 (1995).
[7] M. Honda *et al.*, Nucl. Fusion **46**, 580 (2006).
[8] A. Fukuyama *et al.*, Plasma Phys. Control. Fusion **37**, 611 (1995).
[9] H. Takenaga *et al.*, Nucl. Fusion **43**, 1235 (2003).
[10] J.G. Cordey *et al.*, Nucl. Fusion **43**, 670 (2003).
[11] P.B. Snyder *et al.*, Nucl. Fusion **51**, 102016 (2011).
[12] N. Aiba *et al.*, Comput. Phys. Commun. **175**, 269 (2006).
[13] J.W. Connor, R.J. Hastie and J.B. Taylor, Phys. Rev. Lett. **40**, 396 (1978).
[14] S. Takeji *et al.*, Phys. Plasmas **4**, 4283 (1997).